British Journal of Pharmacology (2005) 144, 28–41
www.nature.com/bjp

Substrate specificity and functional characterisation of the H^+/amino acid transporter rat PAT2 (Slc36a2)

[1]David J. Kennedy, [1]Kelly M. Gatfield, [2]John P. Winpenny, [3]Vadivel Ganapathy & *,[1]David T. Thwaites

[1]Institute for Cell & Molecular Biosciences, Faculty of Medical Sciences, University of Newcastle upon Tyne, Framlington Place, Newcastle upon Tyne NE2 4HH; [2]Biomedicine Group, School of Medicine, Health Policy & Practice, University of East Anglia, Norwich NR4 7TJ and [3]Department of Biochemistry & Molecular Biology, Medical College of Georgia, Augusta, GA 30912-2100, U.S.A.

1 Functional characteristics and substrate specificity of the rat proton-coupled amino acid transporter 2 (rat PAT2 (rPAT2)) were determined following expression in *Xenopus laevis* oocytes using radiolabelled uptake measurements, competition experiments and measurements of substrate-evoked current using the two-electrode voltage-clamp technique. The aim of the investigation was to determine the structural requirements and structural limitations of potential substrates for rPAT2.

2 Amino (and imino) acid transport *via* rPAT2 was pH-dependent, Na^+-independent and electrogenic. At extracellular pH 5.5 (in Na^+-free conditions) proline uptake was saturable (Km 172 ± 41 μM), demonstrating that rPAT2 is, relative to PAT1, a high-affinity transporter.

3 PAT2 preferred substrates are L-α-amino acids with small aliphatic side chains (e.g. the methyl group in alanine) and 4- or 5-membered heterocyclic amino and imino acids such as 2-azetidine-carboxylate, proline and cycloserine, where both D- and L-enantiomers are transported.

4 The major restrictions on transport are side chain size (the ethyl group of α-aminobutyric acid is too large) and backbone length, where the separation of the carboxyl and amino groups by only two CH_2 groups, as in β-alanine, is enough to reduce transport. Methylation of the amino group is tolerated (e.g. sarcosine) but increasing methylation, as in betaine, decreases transport. A free carboxyl group is preferred as *O*-methyl esters show either reduced transport (alanine-*O*-methyl ester) or are excluded.

5 The structural characteristics that determine the substrate specificity of rPAT2 have been identified. This information should prove valuable in the design of selective substrates/inhibitors for PAT1 and PAT2.

British Journal of Pharmacology (2005) **144,** 28–41. doi:10.1038/sj.bjp.0706029

Keywords: Amino acid transport; proton-coupled transport; PAT2; SLC36; Slc36a2; LYAAT; Tramdorin; glycine; cycloserine; neurotransmitter

Abbreviations: ABA, aminobutyric acid; Azet, L-2-azetidine-carboxylate; D-cSer, D-cycloserine; DiMeGly, dimethyl-glycine; D-Pip, D-pipecolic acid; GABA, γ-aminobutyric acid; Isonip, isonipecotic acid; L-cSer, L-cycloserine; L-Pip, L-pipecolic acid; LYAAT-1, lysosomal amino acid transporter 1; MeAIB, methylaminoisobutyric acid; MeAla, *N*-methyl-alanine; MeLeu, *N*-methyl-leucine; mPAT1, mouse proton-coupled amino acid transporter 1; Nip, nipecotic acid; NorLeu, norleucine; NorVal, norvaline; OH-Pro, *trans*-4-hydroxy-proline; *O*-Me-Ala, alanine-*O*-methyl ester; *O*-Me-β-Ala, β-alanine-*O*-methyl ester; *O*-Me-Gly, glycine-*O*-methyl ester; *O*-Me-Pro, proline-*O*-methyl ester; PAT1, proton-coupled amino acid transporter 1; PAT2, proton-coupled amino acid transporter 2; pH_i, intracellular pH; rPAT2, rat proton-coupled amino acid transporter 2; SLC36, solute carrier family 36; Slc36a2, solute carrier family 36 member 2; Tramdorin 1, transmembrane domain-rich protein 1

Introduction

The mammalian genomic information revealed over recent years predicts the expression of many more plasma membrane transport proteins than those detected in functional studies. Previously unidentified transport systems are likely to play fundamental roles in organismal biology. The potential importance of these transporters has been overlooked because of tissue-specific, cell-specific, subcellular or simply low levels of protein expression. Many new transport systems are emerging as potential therapeutic targets for oral drug delivery or treatments for neurological disorders. Only with knowledge of the basic functional characteristics of any particular transport system can the likely physiological or pathophysiological roles of each transport system be predicted and rational approaches to drug design developed.

The first member of solute carrier family 36 (SLC36A1) has been isolated from rat (Sagné *et al*., 2001), mouse (Boll *et al*., 2002) and human (Chen *et al*., 2003a). When expressed in heterologous cell types, SLC36A1 produces a H^+-coupled, pH-dependent, Na^+-independent amino acid transporter, which has been named proton-coupled amino acid transporter 1 (PAT1) (Boll *et al*., 2002; Chen *et al*., 2003a). PAT1 has functional characteristics (Boll *et al*., 2003a; Chen *et al*., 2003a)

*Author for correspondence; E-mail: d.t.thwaites@ncl.ac.uk
Advance online publication: 29 November 2004

identical to the amino acid transport system PAT, previously characterised functionally at the brush-border membrane of the human intestinal epithelial cell line Caco-2 (Thwaites *et al*., 1993a, b; 1994; 1995a–c; 1999; 2000; Thwaites & Stevens, 1999). A transporter with similar functional characteristics has also been identified in rabbit renal brush-border membrane vesicles (Rajendran *et al*., 1987; Roigaard-Petersen *et al*., 1987). PAT1 has recently (Anderson *et al*., 2004) been identified as the transport system which represents the absorptive carrier in the small intestine, previously known as the sarcosine carrier (Newey & Smyth, 1964), the imino acid carrier (Munck, 1966; Munck *et al*., 1994) and the methionine-insensitive sarcosine–glycine–proline system (Thompson *et al*., 1970). Thus, a known transport system, the intestinal H^+-coupled amino acid transporter system PAT (Newey & Smyth, 1964; Munck, 1966; Thompson *et al*., 1970; Thwaites *et al*., 1994; 1995c), has been identified at the molecular level. Although a physiological function for this transporter (amino acid absorption) had been identified at the brush-border membrane of the small intestine, the widespread tissue distribution of PAT1 (at the mRNA level as detected by Northern blot and RT–PCR (Sagné *et al*., 2001; Boll *et al*., 2002; Chen *et al*., 2003a; Anderson *et al*., 2004)) suggests that PAT1 may have previously unidentified functional roles in many other tissues. Indeed rat PAT1/Slc36a1 was isolated from a rat hippocampal cDNA library (Sagné *et al*., 2001). The rat PAT1 clone was originally named lysosomal amino acid transporter 1 (LYAAT-1) because of its lysosomal localisation in the neuronal tissues studied (Sagné *et al*., 2001), although it has also been shown to function in the axonal plasma membrane (Wreden *et al*., 2003). This 'dual' (plasma membrane and intracellular) localisation seems to be common for mammalian H^+-coupled transporters, and has been observed with both the divalent metal transporter DMT1 (Gunshin *et al*., 1997; Cannone-Hergaux *et al*., 1999; Tabuchi *et al*., 2000) and the di/tripeptide transporter PepT1 (Ganapathy & Leibach, 1985; Bockman *et al*., 1997; Walker *et al*., 1998). Thus, a single transport protein may perform separate functions either at different membranes within a single cell type or in different membranes in different cells. The roles of PAT1 in neural tissues are unclear, but are likely to involve movement of neurotransmitters from one compartment to another since both glycine and γ-aminobutyric acid (GABA) are substrates (Sagné *et al*., 2001; Boll *et al*., 2002; Chen *et al*., 2003a; Wreden *et al*., 2003) and PAT1 is expressed in both glutamatergic and GABAergic neurons (Agulhon *et al*., 2003).

The revelation of the PAT1 nucleotide sequence allowed the identification of related sequences and PAT1 is now known to be one of the four members of solute carrier family 36 (SLC36A1-4 or PAT1-4) identified in the mouse, rat and human genomes (Boll *et al*., 2003b; Chen *et al*., 2003b; Bermingham & Pennington, 2004). Interestingly, there is very little evidence in the literature from studies using mammalian tissues for any H^+-coupled amino acid transport function beyond that attributed to PAT1. Thus far PAT2 has been isolated from mouse (Boll *et al*., 2002), rat (Bermingham *et al*., 2002; Chen *et al*., 2003b) and human (Boll *et al*., 2003b). Like PAT1, PAT2 is a H^+/amino acid cotransporter (Boll *et al*., 2002; 2003b; Chen *et al*., 2003b). PAT2 has a much more restricted tissue distribution than PAT1 at the mRNA level and the mRNA seems less abundant, but is found in brain, lung, heart, skeletal muscle and kidney (Bermingham *et al*., 2002; Boll *et al*., 2002; 2003b; Chen *et al*., 2003b). Immunohistochemical studies have localised rat PAT2 (rPAT2) protein to the paranodes and incisures of the sciatic nerve (Bermingham *et al*., 2002). Mouse PAT2 protein is found in both spinal cord and brain where it is localised to the endoplasmic reticulum, recycling endosomes and other cellular compartments, including the plasma membrane (Rubio-Aliaga *et al*., 2004). The role for PAT2 in these tissues remains unclear although the inhibitory neurotransmitter glycine appears to be transported with relatively high affinity.

The purpose of this investigation was to identify the substrate specificity of the rPAT2 transporter by competition studies and measurements of substrate-evoked currents in PAT2-expressing *Xenopus laevis* oocytes. The structural requirements to allow binding of a substrate to PAT2 were determined using a variety of amino acids and derivatives. Only with detailed knowledge of the cellular localisation and substrate specificity of any particular transport system can novel transporters be identified as potential therapeutic targets. The role of this transporter in glycine transport in the CNS is of particular interest since glycine is involved in both postsynaptic inhibition (*via* activation of ligand-gated Cl^- channels) and excitation *via* potentiation of glutamatergic neurotransmission (Lopez-Corcuera *et al*., 2001).

Methods

Materials

L-[2,3-^{3}H]proline (43 Ci mmol^{-1}), L-[4,5-^{3}H]leucine (112 Ci mmol^{-1}), 4-amino-*n*-[2,3-^{3}H]butyric acid (GABA) (81 Ci mmol^{-1}), [2-^{3}H]glycine (16 Ci mmol^{-1}) and [1,2-^{3}H]taurine (29 Ci mmol^{-1}) were from Amersham Biosciences (Little Chalfont, U.K.). α-[*N*-Methyl ^{3}H]methylaminoisobutyric acid (MeAIB) (85 Ci mmol^{-1}), [3-^{3}H(*N*)]β-alanine (50 Ci mmol^{-1}), L-alanine[2,3-^{3}H]methyl ester ([^{3}H]*O*-Me-Ala) (50 Ci mmol^{-1}) and [1-^{14}C]*N*,*N*,*N*-trimethylglycine (betaine) (55 mCi mmol^{-1}) were from American Radiolabeled Chemicals (St Louis, U.S.A.). L-[3-^{3}H]Alanine (74 Ci mmol^{-1}) and L-[3,4-^{3}H]glutamic acid (52 Ci mmol^{-1}) were from NEN Life Sciences (Zaaventem, Belgium). L-[4,5-^{3}H(*N*)]Lysine (99 Ci mmol^{-1}) was from Perkin-Elmer Life Sciences (Boston, U.S.A.). All chemicals including amino acids were of the highest standard available and were purchased from Sigma-Aldrich/Fluka/RBI (Poole, U.K.) or Bachem (St Helens, U.K.).

Functional expression of rPAT2 and mouse PAT1 (mPAT1) in X. laevis *oocytes*

X. laevis oocytes were prepared, and uptake experiments performed, essentially as described previously (Bertran *et al*., 1992; Chen *et al*., 2003b). Individual stage V/VI oocytes were injected with 50 nl of water, rPAT2 (1 μg μl^{-1}) or mPAT1 (1 μg μl^{-1}) cRNA and incubated for 3 days in Barth's solution at 18°C before use. Radiolabelled amino acid uptake (5 μCi ml^{-1}, 0.1–20 mM) was performed in an Na^+-containing or Na^+-free pH 5.0–7.4 buffer (100 mM NaCl or cholineCl, 2 mM KCl, 1 mM $CaCl_2$, 1 mM $MgCl_2$, 10 mM MES (pH 5.0–6.5) or 10 mM HEPES (pH 6.5–7.4), pH adjusted with Tris base) at room temperature (22°C) for 40 min. The substrate

specificity of rPAT2 was investigated by the uptake of a variety of radiolabelled amino acid substrates (all 5 μCi ml^{-1}, 100 μM). In addition, the ability of various amino acids (0.001–20 mM) to compete for [^{3}H]proline or [^{3}H]*O*-Me-Ala (both 5 μCi ml^{-1}, 100 μM) uptake *via* rPAT2 and/or mPAT1 was investigated (with mannitol, used as an osmotic control, being added to each condition so that the final mannitol/amino acid concentration was equivalent). At the end of the incubation period, oocytes were washed three times with 3 ml ice-cold uptake buffer and each oocyte placed in an individual scintillation vial. The oocytes were lysed in 10% SDS prior to addition of 1 ml scintillation cocktail (Perkin-Elmer Life Sciences) and the radioactivity determined by scintillation counting. In the experiments aimed at identifying the functional characteristics of rPAT2, proline was used as the key substrate and proline uptake is expressed as pmol oocyte^{-1} (40 min)$^{-1}$. For comparison of the relative uptake of various radiolabelled amino acids, uptake into rPAT2 or water-injected oocytes is expressed as a % of [^{3}H]proline uptake in rPAT2-injected oocytes. In the competition studies, [^{3}H]proline uptake *via* rPAT2 (or mPAT1) in the presence and absence of unlabelled amino acids (all 10 mM) is expressed as a % control ([^{3}H]proline uptake in the absence of unlabelled amino acid after subtraction of uptake in water-injected oocytes under identical experimental conditions).

Measurement of amino acid-evoked currents using the two-electrode voltage-clamp technique

Two-electrode voltage-clamp experiments were performed on *X. laevis* oocytes, essentially as described previously (Boll *et al*., 2003b). Briefly, *X. laevis* oocytes (prepared as described above, and used 2–4 days post-injection with either 50 nl water, rPAT2 (1 μg μl^{-1}) or mPAT1 (1 μg μl^{-1}) cRNA) were exposed to an extracellular incubation buffer (100 mM cholineCl, 2 mM KCl, 1 mM $CaCl_2$, 1 mM $MgCl_2$, 10 mM MES, pH adjusted to 5.5 with Tris base, 19°C) in an open chamber, while clamped at a membrane potential of −60 mV. Electrodes were fabricated from borosilicate glass and once filled with 3 M KCl gave electrical resistances between 0.5 and 1.5 MΩ. The currents evoked, following addition of various amino acids (all at 10 mM for 120 s) to the solution bathing rPAT2, mPAT1 or water-injected oocytes, were measured as the difference between current measured over a 20 s period before addition of the substrate and the current measured 100–120 s after addition of the substrate. Results are presented both as representative traces and as mean amino acid-evoked current change (following subtraction of current in water-injected control oocytes under identical experimental conditions) and are expressed as a % of current evoked by 10 mM proline.

Statistics

Data are expressed as mean ± s.e.m. (*n*). The *n* number represents the number of individual oocytes per condition. Routinely each experimental condition in the radiolabel uptake experiments is tested using up to 10 oocytes per batch. Each batch of oocytes is from a separate animal. All experiments are performed using oocytes from at least two (up to six) separate batches. Statistical comparisons of mean values were made using one-way analysis of variance (ANOVA) (using the Tukey–Kramer multiple comparisons post-test). One-site hyperbolar and sigmoidal dose–response curves were fitted using GraphPad Prism version 3.00.

Results

Functional characteristics of amino acid transport by rPAT2

Proline (100 μM) uptake into rPAT2-injected oocytes is pH-dependent, being two-fold greater at pH 5.5 compared to pH 7.4 (Figure 1). Under each condition, proline uptake into rPAT2 oocytes is significantly greater than that in water-injected oocytes ($P<0.001$). Three observations in rPAT2-expressing oocytes: (i) no significant difference ($P>0.05$) in proline uptake between pH 5.5 and 7.0; (ii) uptake at pH 7.4 being approximately half maximal; (iii) uptake at pH 7.4 being 10-fold greater than that in water-injected oocytes, suggest that the PAT2 transporter is activated at lower extracellular proton concentrations than PAT1 (Figure 1). In contrast, half-maximal uptake in PAT1-expressing oocytes is observed between pH 6.2 and 6.3 (Figure 1), with a 4.2-fold increase in proline uptake between pH 5.5 and 7.0 ($P<0.001$).

Under all extracellular pH conditions tested, proline uptake by either PAT2 (Figure 2a) or PAT1 (Figure 2b) is Na^+-independent, with no significant difference ($P>0.05$) being observed at pH 5.5, 6.5 or 7.4 in the presence or absence of extracellular Na^+. For the rest of the study, amino acid transport *via* PAT2 was measured under conditions in which PAT2-mediated uptake is optimal (and transport *via* other carriers minimised) using incubation buffers of pH 5.5 and Na^+-free conditions. Under these conditions, proline uptake *via* PAT2 is saturable, with a Km of 172 ± 41 μM (Figure 3).

Substrate selectivity: the effects of methyl substitution on the α carbon and amino group

In Figure 4a, significantly higher uptake of glycine into rPAT2 compared to water-injected oocytes is demonstrated ($P<0.01$).

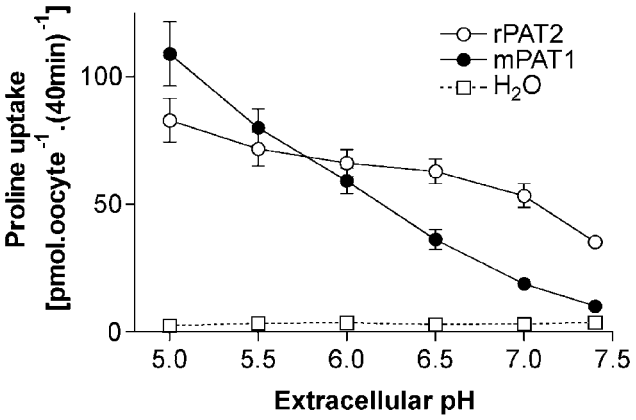

Figure 1 Proline uptake into rPAT2- and mPAT1-expressing *X. laevis* oocytes is dependent upon extracellular pH. Oocytes injected with water (50 nl) are used as a control for expression. Proline (100 μM) uptake was measured for 40 min in Na^+-free conditions (22°C) over the extracellular pH range pH 5.0–7.4. Data are expressed as pmol oocyte^{-1} (40 min)$^{-1}$ and are mean ± s.e.m. ($n=19$–20).

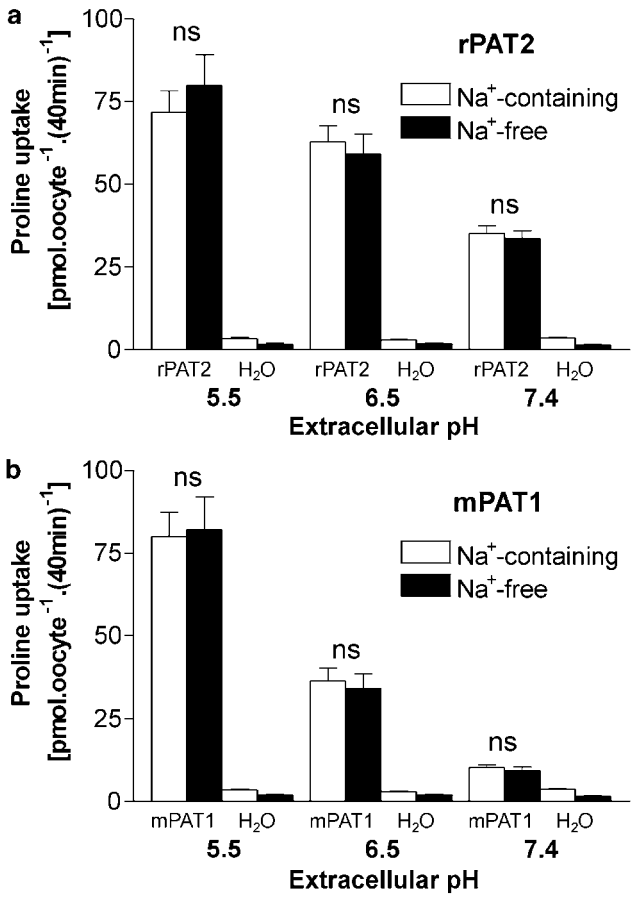

Figure 2 pH-dependent, Na^+-independent, proline uptake into rPAT2- and mPAT1-expressing oocytes. Proline (100 μM) uptake was measured into (a) rPAT2- and (b) mPAT1-expressing oocytes (water-injected oocytes were used as a control) in the presence and absence of extracellular Na^+ at pH 5.5, 6.5 and 7.4. Data are expressed as pmol oocyte^{-1} (40 min)$^{-1}$ and are mean ± s.e.m. (n = 18–20). NS, $P > 0.05$, uptake at each pH in Na^+-containing vs Na^+-free conditions.

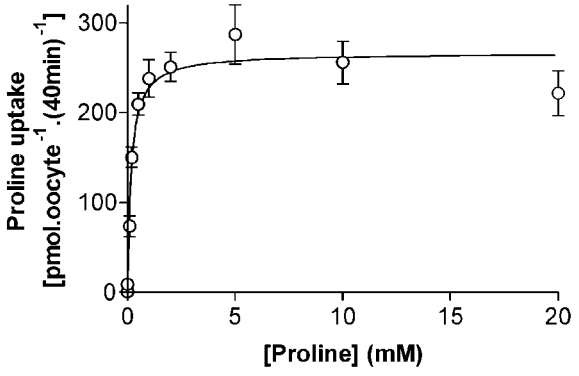

Figure 3 Concentration-dependent proline uptake *via* rPAT2. Proline uptake (pH 5.5, Na^+-free, 40 min) was measured over a range (0.001–20 mM) of proline concentrations into rPAT2-expressing oocytes. Results are expressed following subtraction of uptake into water-injected oocytes, so that the data represent the rPAT2-specific uptake ($r^2 = 0.999$, data fitted using a one-site-binding hyperbola). Data are expressed as pmol oocyte^{-1} (40 min)$^{-1}$ and are mean ± s.e.m. (n = 19–20).

Methyl substitution as observed in alanine (additional methylation of the α-carbon) and MeAIB (both α-carbon and *N*-methylation) does not appear to prevent access to the PAT2 transporter, and, although betaine (trimethyl-glycine) uptake was reduced in comparison with the other substrates, uptake into PAT2 oocytes was 34-fold higher than that in water-injected oocytes (Figure 4a). The ability of a range of methylated compounds (all 10 mM) to inhibit PAT2-mediated proline uptake is demonstrated in Figure 4b. All compounds tested significantly reduced ($P < 0.001$) proline uptake. Addition of a single methyl group on the amino group as in either sarcosine (*N*-methyl glycine) or *N*-methyl-alanine (MeAla) had no effect on the ability of the compound to inhibit proline uptake (Figure 4b). However, additional methylation of the amino group as in dimethyl-glycine (DiMeGly) and betaine did significantly reduce ($P < 0.001$) the level of inhibition of proline uptake compared to that observed with glycine or sarcosine. The level of radiolabelled uptake and pattern of inhibition are closely matched by the ability of each substrate to evoke inward current in PAT2-injected oocytes (Figure 4c–e). No amino acid was able to induce current in water-injected oocytes (Figure 4c and d).

Substrate selectivity: the effects of methyl substitution on the carboxyl group

Alanine, glycine and proline are all good substrates for PAT1 and PAT2 (Figure 4a; Sagné *et al*., 2001; Boll *et al*., 2002; Chen *et al*., 2003a, b). Figure 5a confirms that *O*-methylation of the carboxyl group of alanine, glycine and proline prevents these amino acids accessing PAT1 as all (at 10 mM) are unable to inhibit proline uptake ($P > 0.05$ vs control) (Boll *et al*., 2003a). In contrast, the methyl ester of alanine (*O*-Me-Ala) inhibits [^{3}H]proline uptake *via* PAT2 ($P < 0.05$ vs control) by approximately 50% when tested at a concentration of 10 mM (Figure 5a). At pH 5.5, *O*-Me-Ala will predominantly be in the form of a cation and will thus carry net charge (approximate pK 7.8; Cohn & Edsall, 1943). Figure 5b and c demonstrate that at pH 5.5 *O*-Me-Ala is able to evoke inward current *via* PAT2 (no current is observed in water-injected oocytes; Figure 5b) and that the current is equivalent to that observed with proline, suggesting that the current consists of both the charge carried by the cotransported H^+ and that on the substrate. In contrast, *O*-Me-β-Ala appears not to be a PAT2 substrate as it fails to either inhibit [^{3}H]proline uptake or induce inward current (Figure 5a–c). The observation of *O*-Me-Ala transport *via* rPAT2 was surprising given the lack of transport *via* PAT1. However, the *O*-Me-Ala current evoked *via* rPAT2 at pH 5.5 does appear to be due to substrate transport as there is a 2.7-fold increase in [^{3}H]*O*-Me-Ala uptake into rPAT2 compared to water-injected oocytes (Figure 5d; $P < 0.001$) (in the same oocytes a 13.9-fold increase in proline uptake was observed), which was inhibited by 10 mM proline or *O*-Me-Ala (Figure 5d; both $P < 0.001$ vs control). These observations suggest that, at pH 5.5, *O*-Me-Ala is a substrate for rPAT2. However, at pH 7.4, *O*-Me-Ala also appears to be transported *via* an endogenous oocyte transport system (Figure 5d). When extracellular pH was increased from pH 5.5 to 7.4, there was a 2.9- and 6.0-fold increase in [^{3}H]*O*-Me-Ala uptake in rPAT2 and water-injected oocytes (Figure 5d) (whereas in the same rPAT2-injected oocytes a 50% decrease in proline uptake was observed as pH increased

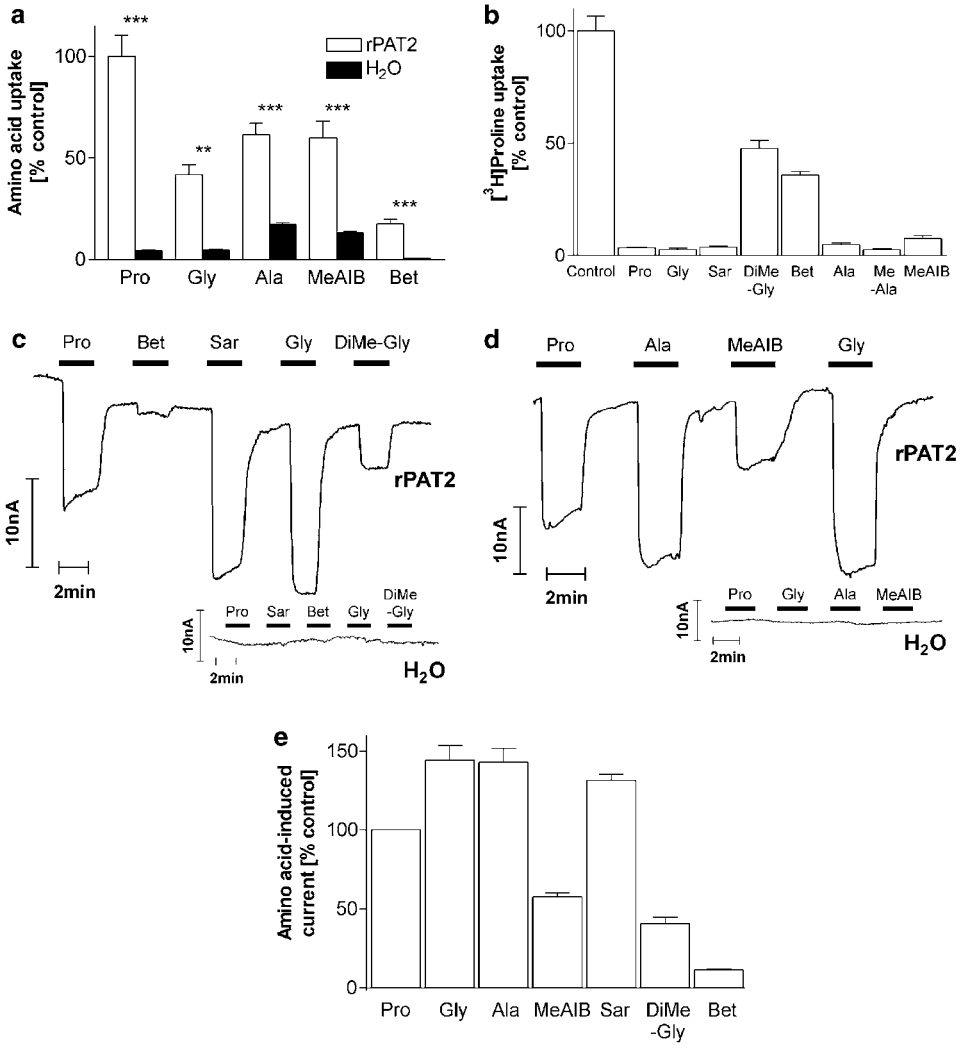

Figure 4 Effects of methylation of the α carbon or amino group on substrate specificity of rPAT2. (a) Uptake of radiolabelled proline (Pro), glycine (Gly), alanine (Ala), MeAIB and betaine (Bet) (all 100 μM, pH 5.5, Na^+-free) into rPAT2 or water-injected oocytes. Data are expressed as a % of [^{3}H]proline uptake in rPAT2-injected oocytes and are mean$\pm$s.e.m. ($n=10$–30). (b) [^{3}H]proline uptake (100 μM, pH 5.5, Na^+-free) *via* rPAT2 in the presence and absence of unlabelled amino acids (all 10 mM). Data are expressed as a % control ([^{3}H]proline uptake in the absence of unlabelled amino acid) after subtraction of uptake in water-injected oocytes under identical experimental conditions. Data are mean$\pm$s.e.m. ($n=19$–60). (c, d) Representative traces showing current changes in rPAT2 and water-injected oocytes following exposure to 10 mM proline, glycine, sarcosine (Sar), DiMe-Gly, betaine, alanine and MeAIB (pH 5.5, Na^+-free conditions) measured using the two-electrode voltage-clamp technique (oocytes clamped at -60 mV). (e) Mean amino acid-evoked current change (as shown in (c, d)) *via* rPAT2 (following subtraction of current in water-injected control oocytes) expressed as a % of current evoked by 10 mM proline. Data are mean$\pm$s.e.m. ($n=4$–11, from four batches). ***$P<0.001$ vs control. **$P<0.01$ vs control.

from pH 5.5 to 7.4, not shown). At pH 7.4, proline (10 mM) inhibited ($P<0.01$) a component of [^{3}H]*O*-Me-Ala uptake in rPAT2-injected oocytes, but had no effect ($P>0.05$) on [^{3}H]*O*-Me-Ala uptake in water-injected oocytes. Unlabelled *O*-Me-Ala (10 mM) had similar inhibitory effects ($P<0.001$) on [^{3}H]*O*-Me-Ala uptake into either rPAT2 or water-injected oocytes (Figure 5d). Thus, at pH 7.4, *O*-Me-Ala appears to be transported both *via* rPAT2 (which is sensitive to proline) and an endogenous transporter, which is insensitive to proline. Figure 5e demonstrates that, at pH 7.4, rPAT2-mediated proline transport is saturated at 10 mM, as there is no increase in proline-evoked current when the extracellular proline concentration is increased from 10 to 20 mM. In contrast, inclusion of 10 mM *O*-Me-Ala, in addition to 10 mM proline, in the extracellular bathing solution is associated with a large current (Figure 5e). This demonstrates that at pH 7.4 *O*-Me-Ala is transported *via* an endogenous (a similar current being observed at pH 7.4 in water-injected oocytes, not shown) electrogenic proline-insensitive transporter, which is inactive at pH 5.5 (Figure 5b). The identity of this endogenous pH-sensitive, Na^+-independent, methylated-amino acid transporter remains unknown.

Substrate selectivity: the effects of backbone length and side chain

Figure 6a shows that there is a 33-fold increase in proline uptake in rPAT2 vs water-injected oocytes ($P<0.001$), whereas

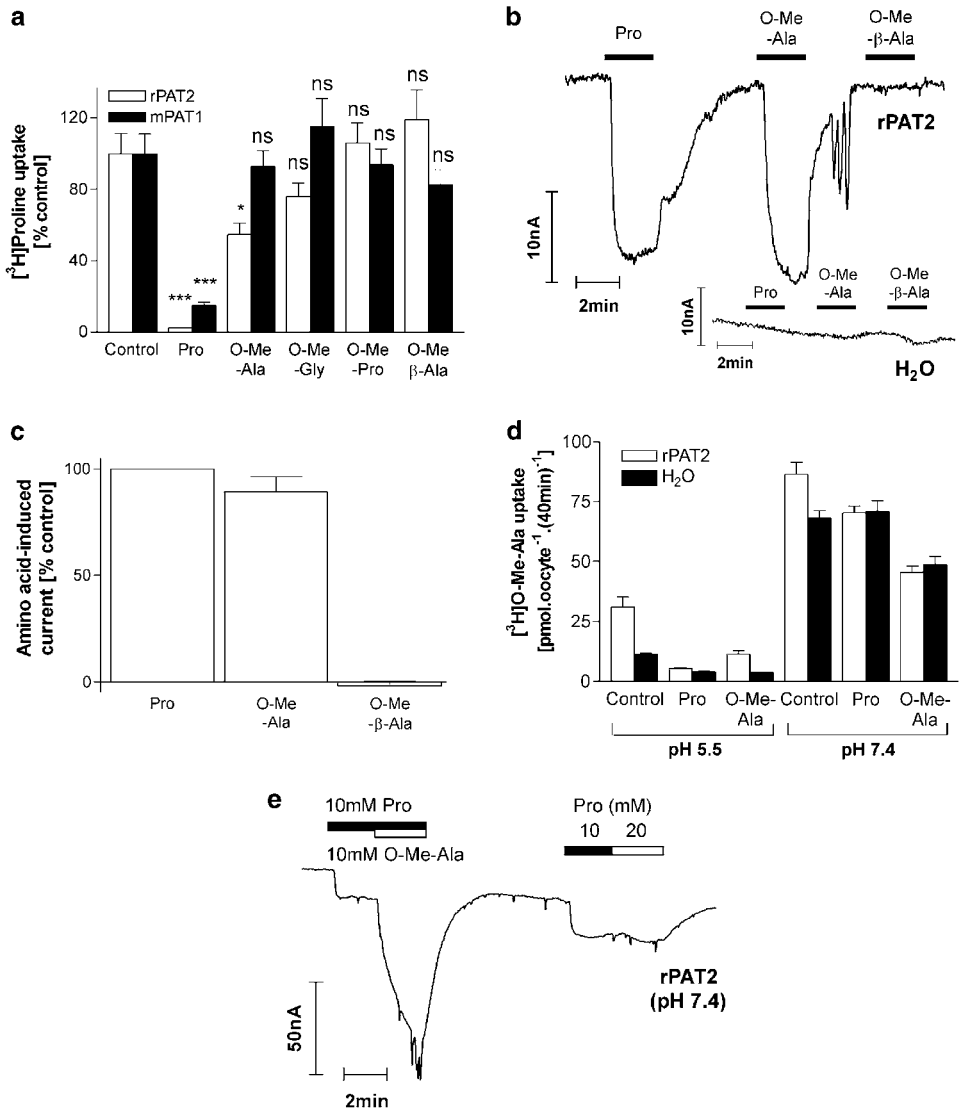

Figure 5 Effects of methylation of the carboxyl group on substrate specificity of rPAT2 (and mPAT1). (a) [^{3}H]proline uptake (100 μM, pH 5.5, Na^+-free) *via* rPAT2 or mPAT1 in the presence and absence of unlabelled proline and *O*-methyl esters of alanine (*O*-Me-Ala), glycine (*O*-Me-Gly), proline (*O*-Me-Pro) and β-alanine (*O*-Me-β-Ala) (all 10 mM). Data are expressed as a % control and are mean $\pm$ s.e.m. ($n = 10$). (b) Representative trace showing current changes in rPAT2 and water-injected oocytes following exposure to 10 mM proline, *O*-Me-Ala and *O*-Me-β-Ala (pH 5.5, Na^+-free conditions). (c) Mean amino acid-evoked current change (as shown in (b)) *via* rPAT2 (following subtraction of current in water-injected control oocytes) expressed as a % of current evoked by 10 mM proline. Data are mean $\pm$ s.e.m. ($n = 5$, from two batches). (d) [^{3}H]*O*-Me-Ala uptake (100 μM, Na^+-free, pH 5.5 and 7.4) in rPAT2 and water-injected oocytes in the presence and absence of unlabelled proline or *O*-Me-Ala (both 10 mM). Results are expressed as mean $\pm$ s.e.m. ($n = 10$). (e) Representative trace (one of three independent experiments) showing current changes in rPAT2-expressing oocytes following exposure to proline (10 and 20 mM) or proline (10 mM) and then proline plus *O*-Me-Ala (both 10 mM). ***$P < 0.001$ vs control. *$P < 0.05$ vs control. NS, $P > 0.05$ vs control.

only a 3.2-, 1.3- and 1.6-fold increase is observed for β-alanine, taurine and GABA (all $P > 0.05$ vs water), respectively, suggesting that increasing the backbone length (and hence distance between the amino and carboxyl groups) is a severe restriction on allowing access of a substrate to PAT2. The data in Figure 6b support this conclusion with β-alanine reducing [^{3}H]proline uptake *via* PAT2 by only 50% ($P < 0.001$) whereas taurine and GABA (all 10 mM) were without effect ($P > 0.05$). In contrast all three compounds significantly reduced ($P < 0.001$) [^{3}H]proline uptake *via* PAT1 (Figure 6b). The ability of each substrate to evoke inward current in PAT2 oocytes (Figure 6c and d) was proportional to the ability of each substrate to inhibit [^{3}H]proline influx (Figure 6b). None of the amino acids had any effect in water injected oocytes (Figure 6c).

One of the interesting features of PAT1 is the ability to discriminate between the α- (α-ABA), β- (β-ABA) and γ- (GABA) forms of aminobutyric acid (Thwaites *et al.*, 2000; Boll *et al.*, 2003a; Anderson *et al.*, 2004). Both GABA and β-ABA are able to significantly ($P < 0.001$) inhibit

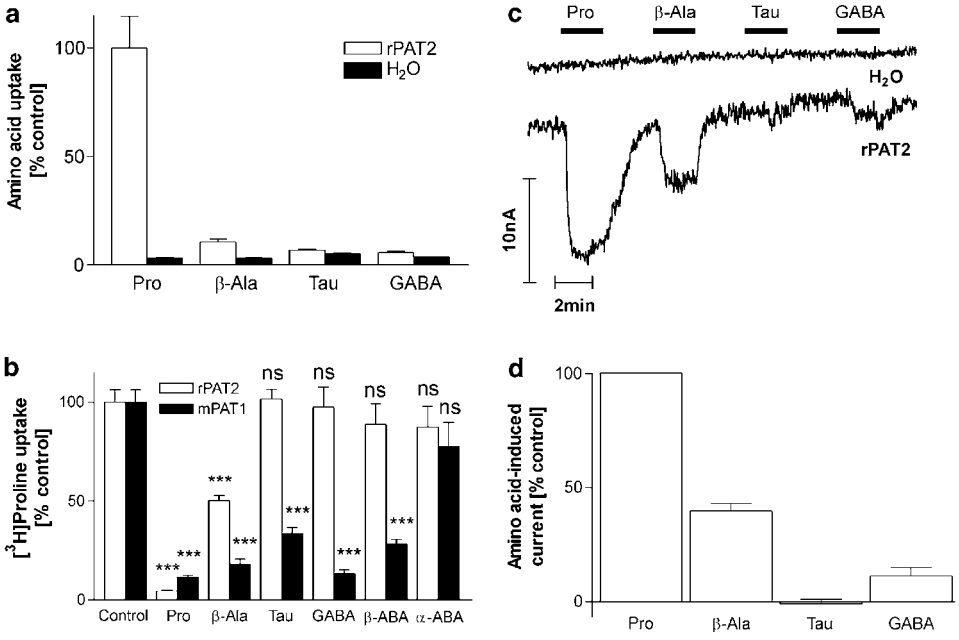

Figure 6 Effects of backbone and side chain length on substrate specificity of rPAT2 (and mPAT1). (a) Uptake of radiolabelled proline, β-alanine, taurine (Tau) and GABA (all 100 μM, pH 5.5, Na^+-free) into rPAT2 or water-injected oocytes. Data are expressed as a % of [^{3}H]proline uptake in rPAT2-injected oocytes and are mean$\pm$s.e.m. ($n=20$). (b) [^{3}H]proline uptake (100 μM, pH 5.5, Na^+-free) *via* rPAT2 and mPAT1 in the presence and absence of the unlabelled amino acids β-alanine, taurine, GABA, β-ABA and α-ABA (all 10 mM). Data are expressed as a % control ([^{3}H]proline uptake in the absence of unlabelled amino acid) after subtraction of uptake in water-injected oocytes under identical experimental conditions. Data are mean$\pm$s.e.m. ($n=9$–49). (c) Representative trace showing current changes in rPAT2 and water-injected oocytes following exposure to 10 mM proline, β-alanine, taurine and GABA (pH 5.5, Na^+-free conditions). (d) Mean amino acid-evoked current change (as shown in (c)) *via* rPAT2 (following subtraction of current in water-injected control oocytes) expressed as a % of current evoked by 10 mM proline. Data are mean$\pm$s.e.m. ($n=5$, from two batches). ***$P<0.001$ vs control. NS, $P>0.05$ vs control.

[^{3}H]proline uptake *via* PAT1 whereas α-ABA is without effect (Figure 6b; $P>0.05$). In contrast all three forms of ABA fail to inhibit [^{3}H]proline uptake *via* PAT2 (Figure 6b; $P>0.05$).

There was no significant difference ($P>0.05$) in uptake of leucine, lysine or glutamate in water and rPAT2-injected oocytes (Figure 7a). Amino acids which have larger side chains either due to branching (leucine and methyl-leucine) or increasing length (norleucine (NorLeu) and norvaline (Nor-Val)) or those including charged groups (the anionic glutamate and cationic lysine) all failed to inhibit [^{3}H]proline uptake *via* rPAT2 (all $P>0.05$ vs control; Figure 7b). Similarly this group of compounds all failed to induce inward current although a small inward current was observed with the cationic amino acid lysine in both water and rPAT2-injected oocytes (Figure 7c and d).

Substrate selectivity: stereoselectivity

Results in Figure 8a and b demonstrate that rPAT2 has a preference for L-alanine compared to D-alanine (Figure 8a; $P<0.05$), with an IC_{50} of 240 μM and 5.5 mM, respectively (Figure 8b). PAT2 does not discriminate between D and L forms of serine (Figure 8a; $P>0.05$), with IC_{50} values >20 mM (Figure 8c). D-Proline at the concentration tested appears to be equipotent ($P>0.05$ for L-proline vs D-proline; Figure 8a) with L-proline, which is broadly similar to observations using PAT1 (Chen *et al*., 2003a). The difference in the ability of PAT1 and PAT2 to distinguish between D and L forms of alanine and serine is demonstrated clearly in Figure 8d–f. Neither D- nor L-cysteine (which have a CH_2SH side chain as opposed to the CH_3 side chain in alanine) are able to inhibit [^{3}H]proline uptake *via* PAT2 ($P>0.05$ vs control; Figure 8a), whereas D-cysteine is a PAT1 substrate (Boll *et al*., 2003a; Chen *et al*., 2003a).

Substrate selectivity: heterocyclic amino and imino acids

A range of heterocyclic amino and imino acids were investigated for their ability to access rPAT2, and, where appropriate, some comparative studies with mPAT1 are presented. It is clear from the results presented previously in this study that the five-membered ring proline is an excellent substrate (in either L or D form), as is the polar hydroxy-proline (Figure 9a, g and h). Both the L and D enantiomers of the five-membered ring cycloserine appear to be high-affinity substrates (Figure 9a, f and h). In PAT2, as in PAT1 (Anderson *et al*., 2004), both D- and L-cycloserine (D- and L-cSer) (both 10 mM) significantly inhibit ($P<0.001$) [^{3}H]proline uptake (Figure 9a), but there does appear to be a preference for the D-enantiomer, which is most evident in the ability of each substrate to stimulate inward current in rPAT2-expressing oocytes (Figure 9f and h). The four-membered ring L-2-azetidine-carboxylate (Azet) significantly inhibits [^{3}H]proline uptake ($P<0.001$) *via* either rPAT2 or mPAT1, suggesting that it is a substrate for both transporters (Figure 9a). Figure 9g and h demonstrates that L-2-azetidine-carboxylate induces inward current *via* rPAT2 ($P>0.05$ vs proline). The results in

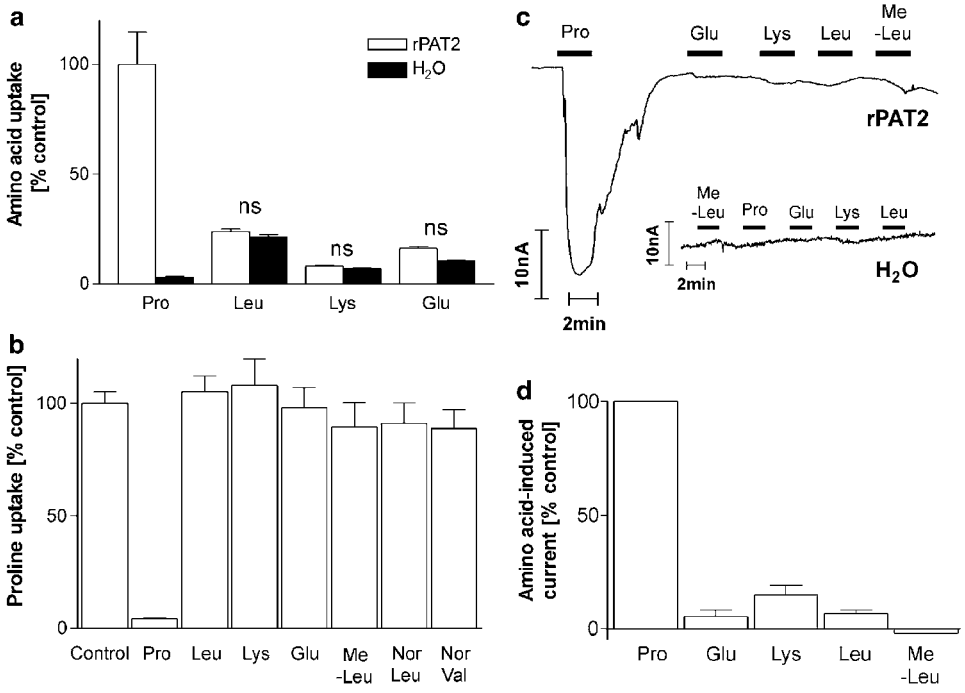

Figure 7 Extension of the amino acid side chain restricts access to rPAT2. (a) Uptake of radiolabelled proline, leucine (Leu), lysine (Lys) and glutamic acid (Glu) (all 100 μM, pH 5.5, Na^+-free) into rPAT2 or water-injected oocytes. Data are expressed as a % of [^{3}H]proline uptake in rPAT2-injected oocytes and are mean $\pm$ s.e.m. ($n = 18$–20). (b) [^{3}H]proline uptake (100 μM, pH 5.5, Na^+-free) *via* rPAT2 in the presence and absence of the unlabelled amino acids proline, leucine, lysine, glutamic acid, MeLeu, NorLeu and NorVal (all 10 mM). Data are expressed as a % control ([^{3}H]proline uptake in the absence of unlabelled amino acid) after subtraction of uptake in water-injected oocytes under identical experimental conditions. Data are mean $\pm$ s.e.m. ($n = 16$–55). (c) Representative traces showing current changes in rPAT2 and water-injected oocytes following exposure to 10 mM proline, glutamic acid, lysine, leucine and methyl-leucine (pH 5.5, Na^+-free conditions). (d) Mean amino acid-evoked current change (as shown in (c)) *via* rPAT2 (following subtraction of current in water-injected control oocytes) expressed as a % of current evoked by 10 mM proline. Data are mean $\pm$ s.e.m. ($n = 5$, from three batches). NS, $P > 0.05$ vs control.

Figure 9a–c confirm and extend our previous observations with mPAT1 (Anderson *et al*., 2004). Figure 9a and b demonstrates that the six-membered ring piperidine carboxylates L- and D-pipecolic acid (L- and D-Pip) (2-piperidine-carboxylate), nipecotic acid (Nip) (3-piperidine-carboxylate) and isonipecotic acid (Isonip) (4-piperidine-carboxylate) all significantly inhibit ($P < 0.001$) mPAT1-mediated [^{3}H]proline influx, but that L-pipecolic acid has the lowest affinity (IC_{50} 16.3 mM) compared to D-pipecolic acid (IC_{50} 6.6 mM) and nipecotic acid (IC_{50} 4.1 mM) (Figure 9b). The relative ability of the substrates to inhibit amino acid transport *via* PAT1 is reflected in their ability to induce current (Figure 9c and h). There is no difference in the current observed upon exposure to isonipecotic acid, nipecotic acid or D-pipecolic acid, whereas the L-pipecolic acid-induced current is smaller (Figure 9c and h; Anderson *et al*., 2004). When the experiments described above for mPAT1 were repeated in the same batches of oocytes with rPAT2, a distinct pattern of substrate selectivity emerged. Figure 9a demonstrates significant inhibition of PAT2-mediated [^{3}H]proline uptake by L-pipecolic acid ($P < 0.001$ vs control), D-pipecolic acid ($P < 0.01$ vs control), nipecotic acid ($P < 0.05$ vs control) and isonipecotic acid ($P < 0.001$; all 10 mM). The inhibition observed with L-pipecolic acid was significantly greater than that observed with D-pipecolic acid ($P < 0.001$ vs L-pipecolic acid), nipecotic acid ($P < 0.001$ vs L-pipecolic acid) or isonipecotic acid ($P < 0.01$ vs L-pipecolic acid; Figure 9a), which is supported by the relative affinity of L-pipecolic acid (IC_{50} 1.2 mM), compared to either D-pipecolic acid (IC_{50} 14.0 mM) or nipecotic ($IC_{50} > 20$ mM) acid (Figure 9d). However, Figure 9e and h demonstrates that for this group of piperidine carboxylates the ability to inhibit PAT2-mediated [^{3}H]proline influx is not correlated with the relative ability to evoke inward current. The currents observed upon exposure to all four compounds were small in comparison to proline, with the surprising observations being that isonipecotic acid evoked the largest current whereas the L-pipecolic acid current was no different from that evoked by either D-pipecolic acid or nipecotic acid.

Discussion

The results in Figure 1 demonstrate differing pH dependence in the functionality of mPAT1 and rPAT2. These differences may relate to the differential cellular and tissue localisation of the two transporters. The half-maximal activity of PAT1 at pH 6.2–6.3 may reflect its expression and activity at the brush border of the small intestine, where its transport activity will be driven partly by the local acid microclimate (Anderson *et al*., 2004). Rubio-Aliaga *et al*. (2004) have recently shown that mPAT2 is most sensitive to changes in extracellular pH between pH 9.0 and 7.5, with half-maximal activation at pH 8.3. Thus, PAT2 is likely to function even in the absence of a

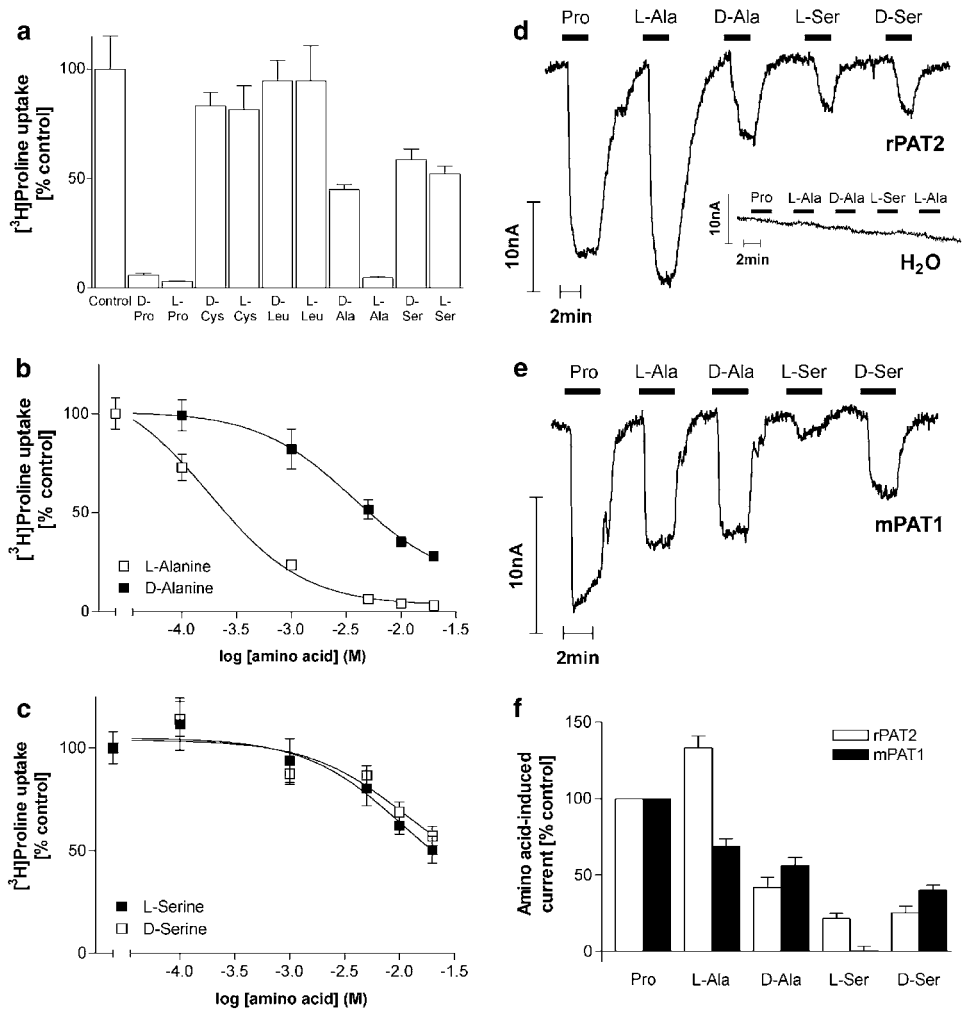

Figure 8 D- and L-amino acids are handled differently by rPAT2 and mPAT1. (a) [^{3}H]proline uptake (100 μM, pH 5.5, Na^+-free) *via* rPAT2 in the presence and absence of the D and L enantiomers of the amino acids proline, cysteine, leucine, alanine and serine (all 10 mM). Data are expressed as a % control ([^{3}H]proline uptake in the absence of unlabelled amino acid) after subtraction of uptake in water-injected oocytes under identical experimental conditions. Data are mean ± s.e.m. ($n = 17$–20). (b) Concentration-dependent inhibition of [^{3}H]proline uptake (100 μM, pH 5.5, Na^+-free) by D- and L-alanine (0.1–20 mM) *via* rPAT2. Data are mean ± s.e.m. ($n = 18$–20), following subtraction of uptake in water-injected oocytes under identical experimental conditions. Data are fitted to sigmoidal dose–response curves, $r^2 = 0.999$ for both curves. (c) Concentration-dependent inhibition of [^{3}H]proline uptake (100 μM, pH 5.5, Na^+-free) *via* rPAT2 by D- and L-serine (0.1–20 mM). Data are mean ± s.e.m. ($n = 18$–20), following subtraction of water-injected controls. Data are fitted to sigmoidal dose–response curves, $r^2 = 0.998$ (L-serine) and $r^2 = 0.993$ (D-serine). (d, e) Representative traces showing current changes in rPAT2 (d), water (d) and mPAT1 (e) injected oocytes following exposure to 10 mM proline, D- and L-alanine and D- and L-serine (pH 5.5, Na^+-free conditions). (f) Mean amino acid-evoked current change (as shown in (d, e)) *via* rPAT2 and mPAT1 (following subtraction of current in water-injected control oocytes) expressed as a % of current evoked by 10 mM proline. Data are mean ± s.e.m. ($n = 4$–7, from three batches).

transmembrane pH gradient and the primary driving force at physiological pH values is likely to be membrane potential rather than the H^+ concentration gradient. The membrane potential sensitivity of mPAT2 was demonstrated recently, with membrane depolarisation being associated with outward amino acid-induced currents, suggesting that the mPAT2 transporter can function in both inward and outward directions depending upon the membrane potential and the combination of substrate and proton concentration gradients (Rubio-Aliaga *et al*., 2004). The observations regarding pH dependence reported here are consistent with studies of mPAT2 expression in oocytes (Boll *et al*., 2002), but contrast with our own previous study of rPAT2 expression in the mammalian cell line human retinal pigment epithelium (HRPE), where the pH profile of PAT2-dependent uptake was more like that observed with PAT1 (Chen *et al*., 2003b). This difference could be due to the expression system used in the various studies, or may suggest that the pH dependence of PAT2 depends upon the local lipid environment or coexpression of accessory proteins.

In previous studies (Thwaites *et al*., 1995c; Boll *et al*., 2003a), a range of substrates were investigated to identify the key structural requirements and structural limitations to determine whether or not an amino acid substrate can access PAT1. Here, the basic structural requirements that allow a substrate to bind to the rPAT2 transporter have been

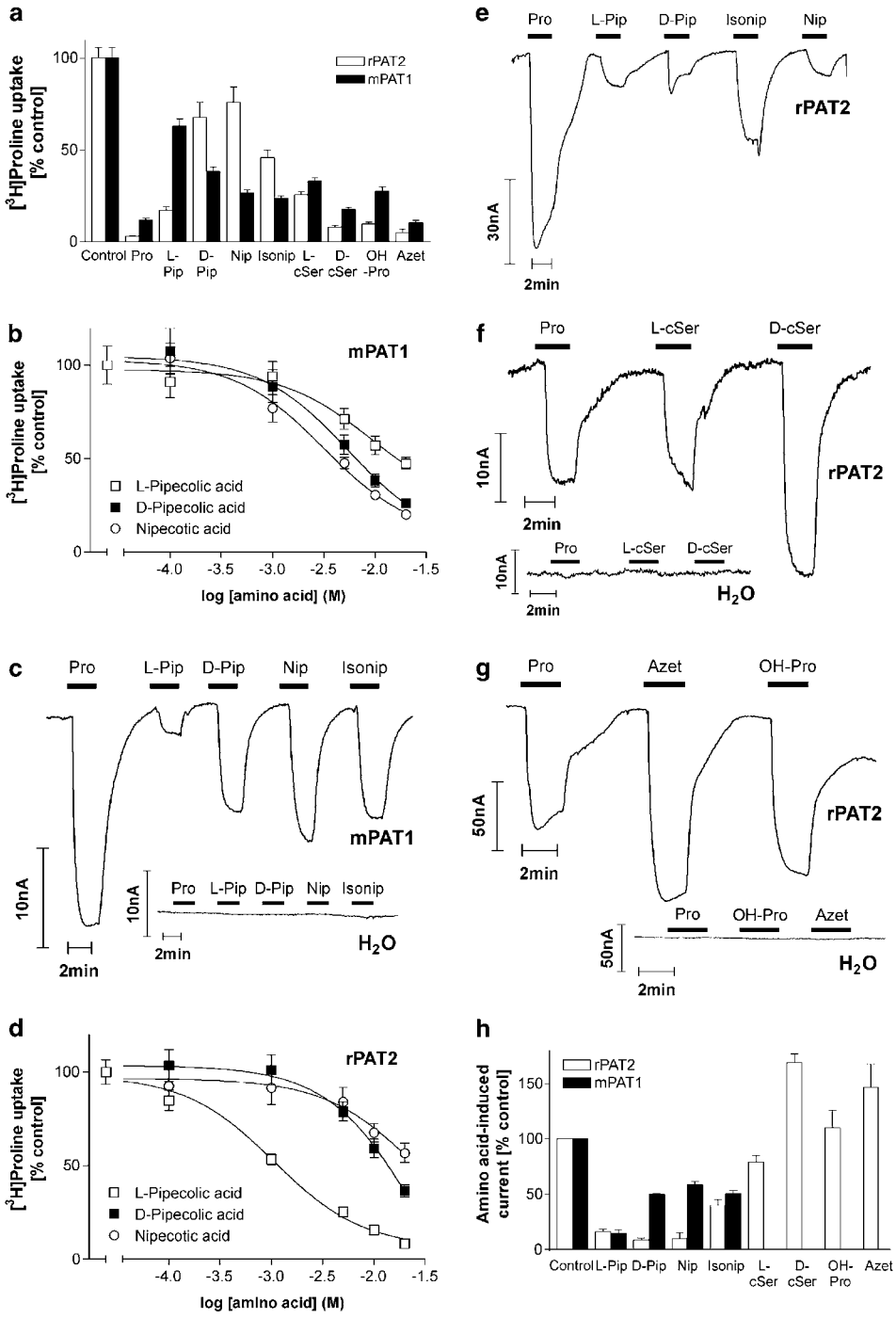

Figure 9 Heterocyclic amino and imino substrates for rPAT2 and mPAT1. (a) [^{3}H]proline uptake (100 μM, pH 5.5, Na$^+$-free) *via* rPAT2 and mPAT1 in the presence and absence of the unlabelled amino acids proline, L- and D-pipecolic acid, (L-Pip and D-Pip), nipecotic acid (Nip), isonipecotic acid (Isonip), L- and D-cycloserine (L-cSer and D-cSer), hydroxy-proline (OH-Pro) and L-2-azetidine-carboxylate (Azet) (all 10 mM). Data are expressed as a % control ([^{3}H]proline uptake in the absence of unlabelled amino acid) after subtraction of uptake in water-injected oocytes under identical experimental conditions. Data are mean$\pm$s.e.m. ($n=20$–59 (rPAT2) and $n=20$–41 (mPAT1)). (b) Concentration-dependent inhibition of [^{3}H]proline uptake (100 μM, pH 5.5, Na$^+$-free) *via* mPAT1 by D- and L-Pip and Nip (0.1–20 mM). Results are expressed as a % control following subtraction of water-injected controls (mean$\pm$s.e.m. ($n=25$–29)). Data are fitted to sigmoidal dose–response curves, $r^2=0.999$ for each curve. (c) Representative trace showing current changes in mPAT1 and water-injected oocytes following exposure to 10 mM proline, L- and D-Pip, Nip and Isonip (pH 5.5, Na$^+$-free conditions). (d) Concentration-dependent inhibition of [^{3}H]proline uptake (100 μM, pH 5.5, Na$^+$-free) *via* rPAT2 by D- and L-Pip and Nip (0.1–20 mM). Results are expressed as a % control following subtraction of water-injected controls (mean$\pm$s.e.m. ($n=27$–28)). Data are fitted to sigmoidal dose–response curves, $r^2=0.999$ for each curve. (e–g) Representative traces showing current changes in rPAT2 and water-injected oocytes following exposure to 10 mM proline, L- and D-Pip, Nip, Isonip, L- and D-cSer, OH-Pro and Azet (all 10 mM). (h) Mean amino acid-evoked current change (as shown in (c), (e–g)) *via* rPAT2 and mPAT1 (following subtraction of current in water-injected control oocytes), expressed as a % of current evoked by 10 mM proline. Data are mean$\pm$s.e.m. ($n=5$, from two batches (mPAT1); $n=5$–7, from four batches (rPAT2)).

identified. Preferred substrates for rPAT2 include small aliphatic amino acids such as glycine and L-alanine, and some heterocyclic amino and imino acids, including D-cycloserine (which binds to the glycine site on the NMDA receptor and which is used in the treatment of schizophrenia (Evins *et al*., 2002) and as an orally delivered antibiotic (Weltman & Rose, 1994)), L-cycloserine (which inhibits tumour (neuroblastoma and medullablastoma) growth *in vitro* (Cinatl *et al*., 1999)) and 2-azetidine-carboxylic acid, which is rich in some higher plants (Romeo, 1989). In general, rPAT2 has a more restricted substrate selectivity compared to mPAT1, and the substrates that are common to both (e.g. glycine, proline) are transported with a much higher affinity by PAT2 than PAT1 (Figure 3).

A key discriminating factor for PAT1 is the site of methyl substitution within the potential amino acid substrate. Figure 4 demonstrates that methylation of the α-carbon (alanine) or amino group (sarcosine) is accepted by rPAT2, with the additional methylation in DiMeGly, betaine and MeAIB reducing apparent affinity without excluding transport. A free carboxyl group appears to be a major requirement for access to the mPAT1 transporter (Boll *et al*., 2003a). Similar observations are found with rPAT2, except that the *O*-methyl ester of alanine (*O*-Me-Ala) is a rPAT2 substrate, as well as a substrate for an endogenous oocyte transport system (Figure 5).

PAT1 accepts not only α amino acids but also amino acid substrates with elongated backbones such as β-alanine, taurine and GABA (Thwaites *et al*., 1993a; 1995c; 2000; Thwaites & Stevens, 1999; Sagné *et al*., 2001; Boll *et al*., 2003a; Anderson *et al*., 2004). In contrast, these compounds are either very poor substrates for PAT2 or are excluded, for example, taurine (Figure 6). Clearly, increasing the backbone length (and hence distance between the amino and carboxyl groups) is a severe restriction on substrate access to PAT2. A key characteristic of PAT1 is the ability to discriminate between the α-, β- and γ- forms of aminobutyric acid (ABA), with β-ABA and GABA being good substrates (Thwaites *et al*., 2000; Boll *et al*., 2003a; Anderson *et al*., 2004). All the three are excluded from PAT2 (Figure 6). The inability of β-ABA to access the PAT2 transporter is presumably due to the increase in backbone length (*via* addition of an additional CH_2 group), since alanine, which has the equivalent CH_3 side chain but no increase in backbone length, is a good substrate (Figure 4). The inability of α-ABA (which, compared to alanine, has an additional CH_2 group in the side chain to form an ethyl group) to access the transporter highlights that the nature of the side chain is one of the major restrictions on substrate access to the PAT2 transport site. Figure 7 demonstrates that any increase in the size of the side chain either due to branching (leucine and methyl-leucine) or increasing length (NorLeu and NorVal) prevents access to PAT2. Amino acids with charged side chains (the anionic glutamate and cationic lysine) are also excluded, but the main reason for this is likely to be the size of the side chain rather than the charge *per se*.

Unlike most other amino acid transporters, PAT1 is unusual in that it has a preference for some amino acids (e.g. serine, cysteine, pipecolate and ABA) in the form of the D rather than L enantiomer, whereas it does not discriminate between the D and L forms of alanine and proline (Thwaites *et al*., 1995c; 2000; Boll *et al*., 2002; 2003a; Chen *et al*., 2003a; Anderson *et al*., 2004). In contrast, rPAT2 does not discriminate between the D and L forms of proline and serine, but has a preference for L- over D-alanine (Figure 8). Neither D- nor L-cysteine (which have a CH_2SH side chain as opposed to the CH_3 side chain in alanine) are substrates for PAT2, which suggests that there is an even greater restriction (compared to PAT1) in the transporter-binding pocket in relation to the bulkiness of the side chain. The polarity of the thiol group in cysteine may be a limiting factor, although the hydroxyl group in serine appears better (relatively) tolerated.

A number of pharmacologically neuroactive heterocyclic compounds are excellent PAT1 substrates (Ranaldi *et al*., 1994; Thwaites *et al*., 1995a; 2000; Anderson *et al*., 2004). In the five-membered ring of proline, the imino nitrogen is not free but is rather attached to the side chain. For proline to be a substrate for PAT2, it appears that the transporter must recognise the imino group as separated by only a single carbon (the α carbon) from the carboxyl group. Thus, although in proline both the side chain and the separation of imino and carboxyl groups (if the imino group is viewed as being on the δ carbon in relation to the carboxyl group) are potentially greater in size and length than those predicted for a transported substrate (and even excluded substrates such as α-ABA and GABA, respectively), it is clear from the results presented in this study that proline is an excellent substrate (in either L or D form), as is the polar hydroxy-proline (Figure 9a, g and h). The five-membered ring cycloserine (in either L or D forms) is an excellent PAT2 substrate. As in proline, the charged groups in cycloserine are separated only by the α carbon, but the amino group is not contained within the ring structure. The four-membered ring L-2-azetidine-carboxylate, another excellent PAT2 substrate, contains the imino group within the ring structure, but as in proline the imino and carboxyl groups are separated only by the α carbon. In general, the ability of each substrate to compete with [^{3}H]proline for transport *via* PAT2 was matched closely with the relative ability to induce inward current in PAT2-expressing oocytes. However, this relationship for rPAT2 is not apparent for the series of six-membered ring piperidine carboxylates, pipecolic acid, nipecotic acid and isonipecotic acid, which differ only by the position of the imino group within the ring relative to the carboxyl group. We have previously demonstrated that the endogenous hPAT1 transporter in human intestinal epithelial Caco-2 cell monolayers functions in a similar manner, with regard to substrate specificity of heterocyclic compounds, as either the hPAT1 or mPAT1 clones, following expression in *X. laevis* oocytes (Thwaites *et al*., 2000; Anderson *et al*., 2004). Thus, PAT1 accepts heterocyclic amino acid substrates, but does not distinguish clearly between substrates where the imino group is, relative to the carboxyl group, in either the α- (at least in D-pipecolic acid, although L-pipecolic acid has the lowest affinity of the group), β- (nipecotic acid) or γ- (isonipecotic acid) positions within the six-membered ring. The separation of charged groups in isonipecotic acid is analogous to the backbone length in GABA; so it is not surprising that isonipecotic acid is a substrate for PAT1 (although by the same rule it should not be, but clearly is, a low-affinity substrate for rPAT2; Figure 9a, e and h). The preference for D- over L-pipecolate may reflect a broad characteristic of PAT1 (as observed also for serine, cysteine and ABA; Thwaites *et al*., 1995c; 2000; Boll *et al*., 2002; 2003a; Chen *et al*., 2003a; Anderson *et al*., 2004) or the ability of the transporter to recognise heterocyclic compounds, not due to low or weak stereospecificity, but rather due to a distinction in the form of recognition of the two isomers (Christensen *et al*.,

1994). Christensen *et al*. (1994) suggested that, in the case of heterocyclic compounds, for example, proline, the single imino and carboxyl groups could be recognised by two distinct separations, so that when L-proline is viewed as a δ- rather than α-imino acid it could perhaps also be recognised as a D-imino acid. Dual modes of enantiorecognition in the binding sites of both PAT1 and PAT2 may be possible. The observation that L-pipecolic acid is apparently a better inhibitor than transported substrate, in contrast to both D-pipecolic acid and nipecotic acid, which are poor inhibitors and poorly transported, in rPAT2 (whereas in mPAT1 there is a close correlation between transport and inhibition) suggest that the structure of L-pipecolic acid could provide a lead compound for the design of pharmacological tools to act as selective inhibitors of PAT2 and PAT1.

The physiological (or pathophysiological) role played by this transporter remains to be elucidated although localisation of mPAT2 RNA and protein to the spinal cord and brain (Rubio-Aliaga *et al*., 2004) suggests that PAT2 may play a role in the control of neurotransmitter transport and in particular a role in the transmembrane movement of glycine. Glycine is involved in both postsynaptic inhibition (*via* activation of ligand-gated Cl^- channels) and excitation *via* potentiation of glutamatergic neurotransmission (Lopez-Corcuera *et al*., 2001). In general, mPAT2 immunoreactivity in mouse brain has a differential expression pattern compared to marker proteins for the glycinergic and GABAergic systems (Rubio-Aliaga *et al*., 2004), suggesting that mPAT2 is not involved in glycine movement at inhibitory synapses. The lack of association with GABAergic regions of the brain is perhaps not surprising when considered alongside the weak affinity of PAT2 for GABA and related compounds such as the GABA uptake inhibitor nipecotic acid (Krogsgaard-Larsen *et al*., 1987). mPAT2 immunoreactivity is found solely in neurones, and not in astrocytes, and is colocalised in neurones positive for the NMDA receptor subunit NR1 (Rubio-Aliaga *et al*., 2004). At the subcellular level, in the spinal cord, mPAT2 protein is found predominantly in endoplasmic reticulum (34%) and recycling endosomes (31%) and also in other cell compartments, including the cell membrane (Rubio-Aliaga *et al*., 2004). This distribution is similar to that following transfection of mPAT2 into HeLa cells, where mPAT2 is found in the plasma membrane and other intracellular compartments but is absent from lysosomes (Boll *et al*., 2002). Similarly, in rat sciatic nerve, rPAT2 (Tramdorin 1) immunoreactivity is absent from lysosomes (Bermingham *et al*., 2002). Cell surface expression of mPAT2 and colocalisation with an NMDA receptor subunit suggest a potential role for PAT2 at glutamatergic synapses, where glycine acts as a coagonist on the NMDA receptor, a function that is mimicked by the rPAT2 substrate D-cycloserine. Thus, PAT2 may play a role in amino acid influx and efflux across the neuronal cell membrane. Glycine influx by rat CNS tissues has been measured in a number of studies. Johnston & Iversen (1971) identified that glycine uptake into rat cerebral cortex slices or homogenates was *via* a low-affinity system with a Km of 264–300 μM, whereas a high-affinity mechanism was present in the spinal cord (Km 36 μM). A series of studies by Snyder and colleagues (e.g. Logan & Snyder, 1971; Bennett *et al*., 1974) demonstrated that the low-affinity uptake mechanism for glycine in rat synaptosomes was present in both cerebral cortex (Km 763 μM) and spinal cord (923 μM). In addition, alanine was transported with similar affinity (453–1058 μM) to glycine (Logan & Snyder, 1971) and in purified synaptosomes a proportion of uptake of glycine (51%), alanine (49%) and proline (26%) was Na^+-independent. The high-affinity system in these studies can be accounted for by the high-affinity Na^+- and Cl^--dependent transporters GLYT1 and GLYT2 (for a review, see Lopez-Corcuera *et al*., 2001). The low-affinity system has not been identified, although Rubio-Aliaga *et al*. (2004) have recently suggested that PAT2 could represent this low-affinity, Na^+-independent uptake mechanism for glycine. The low-affinity glycine uptake in rat brain (Km 264–923 μM) is close to the affinity of rPAT2 for glycine, determined following expression in either HRPE cells (Km 486 μM) or *X. laevis* oocytes (691 μM) (Chen *et al*., 2003b). Since mPAT2 functions bidirectionally, and efflux is increased following membrane depolarisation, PAT2 may also play a role in amino acid efflux (Rubio-Aliaga *et al*., 2004), which could allow efflux of intracellular glycine following glutamate activation of the NMDA receptor, which in turn would potentiate the excitatory response. This role for PAT2 in glycine efflux might be particularly relevant at glutamatergic synapses where neither glycine vesicular release nor the vesicular transporter VGAT have been identified (Chaudry *et al*., 1998; Lopez-Corcuera *et al*., 2001). The relative low affinity of PAT2 for uptake of D-serine, considered to be the endogenous ligand for the glycine site on the NMDA receptor, may also help potentiate the excitatory response by maintaining extracellular levels of D-serine released from the astrocytes (Baranano *et al*., 2001).

The only other potential physiological role for PAT2 suggested to date is in the supply of amino acid substrates to myelinating Schwann cells. Rat PAT2 (Tramdorin 1) gene expression is reduced in the absence of the POU domain transcription factor pou3f1, which is required for differentiation of myelinating Schwann cells (Bermingham *et al*., 2002). However, there is some pharmacological relevance to this observation as the rPAT2 substrate L-cycloserine is a potent inhibitor of palmitoylserine transferase, which is the first enzyme of the sphingolipid pathway (Cinatl *et al*., 1999). In rats, *in vivo* L-cycloserine reduces myelin sheet thickness (Oshida *et al*., 2003) and decreases the cerebroside (a metabolite of sphingolipids used as a marker of myelination in vertebrates) and galactosylceramide content of myelin (Miller & Denisova, 1998). Thus, PAT2 may provide a pathway for entry of L-cycloserine into myelinating cells such as Schwann cells. L-cycloserine has been used in the twitcher mouse model of globoid cell leukodystrophy (also known as Krabbe disease and which is an autosomal recessive disorder of the gene for galactosylceramidase) to reduce psychosine levels in the pons and medulla (Biswas *et al*., 2003). A reduction in galactosylceramidase activity leads to a build-up of the toxic psychosine in Schwann cells and L-cycloserine could be used in substrate reduction therapy to slow the rate of production of the substrates for the defective enzyme (Biswas *et al*., 2003).

In conclusion, we have identified the basic structural requirements that allow an amino acid substrate to access the rPAT2 transport system. Further detailed kinetic analysis is required to develop a substrate-binding model to determine how compounds containing distinct structural features interact with the transporter, which will help distinguish between apparent changes in substrate affinity and effects on transport capacity. The ability of a number of neuroactive compounds to access this transport system, when considered alongside the

tissue and cellular distribution (Rubio-Aliaga *et al*., 2004), suggest that this transporter could play an important role in the control of synaptic levels of amino acids involved in neurotransmission. Only with detailed knowledge of the cellular localisation and substrate specificity of any particular transport system can novel transporters be identified as potential therapeutic targets. Thus, potential physiological and pharmacological roles for PAT2 have been identified and the relevance to previous studies using mammalian brain acknowledged. Along with the numerous other transport systems expressed in mammalian brain, PAT2 could prove to be an important target for future strategies aimed at the design of drugs to target various neurological disorders with L-pipecolate, providing a potential lead compound for the design of a specific PAT2 substrate or inhibitor.

This study was supported by an MRC Career Establishment grant (G9801704) and a BBSRC project grant (13/D17277) to D.T.T. K.M.G. was supported by a BBSRC Postgraduate Studentship. We thank Dr C.M.H. Anderson for helpful discussion and comments on the manuscript. Mouse PAT1 was a gift from Dr M. Boll (Freising-Weihenstephan, Germany).

References

AGULHON, C., ROSTAING, P., RAVASSARD, P., SAGNÉ, C., TRILLER, A. & GIROS, B. (2003). Lysosomal amino acid transporter LYAAT-1 in the rat central nervous system: an *in situ* hybridization and immunohistochemical study. *J. Comp. Neurol.,* **462,** 71–89.

ANDERSON, C.M.H., GRENADE, D.S., BOLL, M., FOLTZ, M., WAKE, K.A., KENNEDY, D.J., MUNCK, L.K., MIYAUCHI, S., TAYLOR, P.M., CAMPBELL, F.C., MUNCK, B.G., DANIEL, H., GANAPATHY, V. & THWAITES, D.T. (2004). H^+/amino acid transporter 1 (PAT1) is the 'imino acid carrier': an intestinal nutrient/drug transporter in human and rat. *Gastroenterology,* **127,** 1410–1422.

BARANANO, D.E., FERRIS, C.D. & SNYDER, S.H. (2001). Atypical neural messengers. *Trends Neurosci.,* **24,** 99–106.

BENNETT, J.P., MULDER, A.H. & SNYDER, S.H. (1974). Neurochemical correlates of synaptically active amino acids. *Life Sci.,* **15,** 1045–1056.

BERMINGHAM, J.R. & PENNINGTON, J. (2004). Organization and expression of the SLC36 cluster of amino acid transport genes. *Mamm. Genome,* **14,** 114–125.

BERMINGHAM, J.R., SHUMAS, S., WHISENHUNT, T., SIRKOWSKI, E.E., O'CONNELL, S., SCHERER, S.S. & ROSENFELD, M.G. (2002). Identification of genes that are downregulated in the absence of the POU domain transcription factor pou3f1 (Oct-6, Tst-1, SCIP) in sciatic nerve. *J. Neurosci.,* **22,** 10217–10231.

BERTRAN, J., WERNER, A., STANGE, G., MARKOVICH, D., BIBER, J., TESTAR, X., ZORZANO, A., PALACIN, M. & MURER, H. (1992). Expression of Na^+-independent amino acid transport in *Xenopus laevis* oocytes by injection of rabbit kidney cortex mRNA. *Biochem. J.,* **281,** 717–723.

BISWAS, S., BIESIADA, H., WILLIAMS, T.D. & LEVINE, S.M. (2003). Substrate reduction intervention by l-cycloserine in Twitcher Mice (globoid cell leukodystrophy) on a B6;CAST/Ei background. *Neurosci. Lett.,* **347,** 33–36.

BOCKMAN, D.E., GANAPATHY, V., OBLAK, T.G. & LEIBACH, F.H. (1997). Localization of peptide transporter in nuclei and lysosomes of the pancreas. *Int. J. Pancreatol.,* **22,** 221–225.

BOLL, M., FOLTZ, M., ANDERSON, C.M.H., OECHSLER, C., KOTTRA, G., THWAITES, D.T. & DANIEL, H. (2003a). Substrate recognition by the mammalian proton-dependent amino acid transporter PAT1. *Mol. Membr. Biol.,* **20,** 261–269.

BOLL, M., FOLTZ, M., RUBIO-ALIAGA, I. & DANIEL, H. (2003b). A cluster of proton/amino acid transporter genes in the human and mouse genomes. *Genomics,* **82,** 47–56.

BOLL, M., FOLTZ, M., RUBIO-ALIAGA, I., KOTTRA, G. & DANIEL, H. (2002). Functional characterization of two novel mammalian electrogenic proton-dependent amino acid cotransporters. *J. Biol. Chem.,* **277,** 22966–22973.

CANNONE-HERGAUX, F., GRUENHEID, S., PONKA, P. & GROS, P. (1999). Cellular and subcellular localization of the Nramp2 iron transporter in the intestinal brush border and regulation by dietary iron. *Blood,* **93,** 4406–4417.

CHAUDRY, F.A., REIMER, R.J., BELLOCCHIO, E.E., DANBOLT, N.C., OSEN, K.K., EDWARDS, R.H. & STORM-MATHISEN, J. (1998). The vesicular GABA transporter, VGAT, localizes to synaptic vesicles in sets of glycinergic as well as GABAergic neurons. *J. Neurosci.,* **18,** 9733–9750.

CHEN, Z., FEI, Y.J., ANDERSON, C.M.H., WAKE, K.A., MIYAUCHI, S., HUANG, W., THWAITES, D.T. & GANAPATHY, V. (2003a). Structure, function and immunolocalization of a proton-coupled amino acid transporter (hPAT1) in the human intestinal cell line Caco-2. *J. Physiol.,* **546,** 349–361.

CHEN, Z., KENNEDY, D.J., WAKE, K.A., ZHUANG, L., GANAPATHY, V. & THWAITES, D.T. (2003b). Structure, tissue expression pattern, and function of the amino acid transporter rat PAT2. *Biochem. Biophys. Res. Commun.,* **304,** 747–754.

CHRISTENSEN, H.N., GREENE, A.A., KAKUDA, D.K. & MACLEOD, C.L. (1994). Special transport and neurological significance of two amino acids in a configuration conventionally designated as D. *J. Exp. Biol.,* **196,** 297–305.

CINATL JR, J., CINATL, J., KOTCHETKOV, R., POUCKOVA, P., VOGEL, J.U., RABINEAU, H., MICHAELIS, M. & KORNHUBER, B. (1999). Cytotoxicity of L-cycloserine against human neuroblastoma and medulloblastoma cells is associated with the suppression of ganglioside expression. *Anticancer Res.,* **19,** 5349–5354.

COHN, E.J. & EDSALL, J.T. (1943). *Proteins, Amino Acids and Peptides as Ions and Dipolar Ions.* New York: Reinhold Publishing Corporation.

EVINS, A.E., AMICO, E., POSEVER, T.A., TOKER, R. & GOFF, D.C. (2002). D-cycloserine added to risperidone in patients with primary negative symptoms of schizophrenia. *Schizophrenia Res.,* **56,** 19–23.

GANAPATHY, V. & LEIBACH, F.H. (1985). Is intestinal peptide transport energized by a proton gradient? *Am. J. Physiol.,* **249,** G153–G160.

GUNSHIN, H., MACKENZIE, B., BERGER, U.V., GUNSHIN, Y., ROMERO, M.F., BORON, W.F., NUSSBERGER, S., GOLLAN, J.L. & HEDIGER, M.A. (1997). Cloning and characterization of a mammalian proton-coupled metal ion transporter. *Nature,* **388,** 482–488.

JOHNSTON, G.A.R. & IVERSEN, L.L. (1971). Glycine uptake in rat central nervous system slices and homogenates: evidence for different uptake systems in spinal cord and cerebral cortex. *J. Neurochem.,* **18,** 1951–1961.

KROGSGAARD-LARSEN, P., FALCH, E., LARSSON, O.M. & SCHOUSBOE, A. (1987). GABA uptake inhibitors: relevance to antiepileptic drug research. *Epilepsy Res.,* **1,** 77–93.

LOGAN, W.J. & SNYDER, S.H. (1971). Unique high affinity uptake systems for glycine, glutamic and aspartic acids in central nervous tissue of the rat. *Nature,* **234,** 297–299.

LOPEZ-CORCUERA, B., GEERLINGS, A. & ARAGORN, C. (2001). Glycine neurotransmitter transporters: an update. *Mol. Membr. Biol.,* **18,** 13–20.

MILLER, S.L. & DENISOVA, L. (1998). Cycloserine-induced decrease of cerebroside in myelin. *Lipids,* **33,** 441–443.

MUNCK, B.G. (1966). Amino acid transport by the small intestine of the rat. *Biochim. Biophys. Acta,* **120,** 97–103.

MUNCK, B.G., MUNCK, L.K., RASMUSSEN, S.N. & POLACHE, A. (1994). Specificity of the imino acid carrier in rat small intestine. *Am. J. Physiol.,* **266,** R1154–R1161.

NEWEY, H. & SMYTH, D.H. (1964). The transfer system for neutral amino acids in the rat small intestine. *J. Physiol.,* **170,** 328–343.

OSHIDA, K., SHIMIZU, T., TAKASE, M., TAMURA, Y., SHIMIZU, T. & YAMASHIRO, Y. (2003). Effects of dietary sphingomyelin on central nervous system myelination in developing rats. *Pediatr. Res.,* **53,** 589–593.

RAJENDRAN, V.M., BARRY, J.A., KLEINMAN, J.G. & RAMASWAMY, K. (1987). Proton gradient dependent transport of glycine in rabbit renal brush border membrane vesicles. *J. Biol. Chem.,* **262,** 14974–14977.

RANALDI, G., ISLAM, K. & SAMBUY, Y. (1994). D-cycloserine uses an active transport mechanism in the human intestinal cell line Caco-2. *Antimicrob. Agents Chemother.,* **38,** 1239–1245.

ROIGAARD-PETERSEN, H., JACOBSEN, C. & SHEIKH, M.I. (1987). H^+-L-proline cotransport by vesicles from pars convoluta of rabbit proximal tubule. *Am. J. Physiol.,* **253,** F15–F20.

ROMEO, J.T. (1989). Heterocyclic amino acids (iminosine, azetidine-2-carboxylic acid, pipecolic acid). In: *Toxicants of Plant Origins,* ed. P.R. Cheeke. pp. 125–139. Orlando: CRC Press.

RUBIO-ALIAGA, I., BOLL, M., VOGT WEISENHORN, D.M., FOLTZ, M., KOTTRA, G. & DANIEL, H. (2004). The proton/amino acid cotransporter PAT2 is expressed in neurons with a different subcellular localization than its paralog PAT1. *J. Biol. Chem.,* **279,** 2754–2760.

SAGNÉ, C., AGULHON, C., RAVASSARD, P., DARMON, M., HAMON, M., EL MESTIKAWY, S., GASNIER, B. & GIROS, B. (2001). Identification and characterization of a lysosomal transporter for small neutral amino acids. *Proc. Natl. Acad. Sci. U.S.A.,* **98,** 7206–7211.

TABUCHI, M., YOSHIMORI, T., YAMAGUCHI, K., YOSHIDA, T. & KISHI, F. (2000). Human NRAMP2/DMT1, which mediates iron transport across endosomal membranes, is localized to late endosomes and lysosomes in HEp-2 cells. *J. Biol. Chem.,* **275,** 22220–22228.

THOMPSON, E., LEVIN, R.J. & JACKSON, M.J. (1970). The stimulating effect of low pH on the amino acid transferring systems of the small intestine. *Biochim. Biophys. Acta,* **196,** 120–122.

THWAITES, D.T., ARMSTRONG, G., HIRST, B.H. & SIMMONS, N.L. (1995a). D-Cycloserine transport in human intestinal epithelial (Caco-2) cells: mediation by a H^+-coupled amino acid transporter. *Br. J. Pharmacol.,* **115,** 761–766.

THWAITES, D.T., BASTERFIELD, L., MCCLEAVE, P.M.J., CARTER, S.M. & SIMMONS, N.L. (2000). Gamma-aminobutyric acid (GABA) transport across human intestinal epithelial (Caco-2) cell monolayers. *Br. J. Pharmacol.,* **129,** 457–464.

THWAITES, D.T., FORD, D., GLANVILLE, M. & SIMMONS, N.L. (1999). H^+/solute-induced intracellular acidification leads to selective activation of apical Na^+/H^+ exchange in human intestinal epithelial cells. *J. Clin. Invest.,* **104,** 629–635.

THWAITES, D.T., MCEWAN, G.T.A., BROWN, C.D.A., HIRST, B.H. & SIMMONS, N.L. (1993a). Na^+-independent, H^+-coupled transepithelial β-alanine absorption by human intestinal Caco-2 cell monolayers. *J. Biol. Chem.,* **268,** 18438–18441.

THWAITES, D.T., MCEWAN, G.T.A., BROWN, C.D.A., HIRST, B.H. & SIMMONS, N.L. (1994). L-Alanine absorption in human intestinal cells driven by the proton electrochemical gradient. *J. Membr. Biol.,* **140,** 143–151.

THWAITES, D.T., MCEWAN, G.T.A., COOK, M.J., HIRST, B.H. & SIMMONS, N.L. (1993b). H^+-coupled (Na^+-independent) proline transport in human intestinal (Caco-2) epithelial cell monolayers. *FEBS Lett.,* **333,** 78–82.

THWAITES, D.T., MCEWAN, G.T.A., HIRST, B.H. & SIMMONS, N.L. (1995b). H^+-coupled α-methylaminoisobutyric acid transport in human intestinal Caco-2 cells. *Biochim. Biophys. Acta,* **1234,** 111–118.

THWAITES, D.T., MCEWAN, G.T.A. & SIMMONS, N.L. (1995c). The role of the proton electrochemical gradient in the transepithelial absorption of amino acids by human intestinal Caco-2 cell monolayers. *J. Membr. Biol.,* **145,** 245–256.

THWAITES, D.T. & STEVENS, B.C. (1999). H^+/zwitterionic amino acid symport at the brush-border membrane of human intestinal epithelial (Caco-2) cells. *Exp. Physiol.,* **84,** 275–284.

WALKER, D., THWAITES, D.T., SIMMONS, N.L., GILBERT, H.J. & HIRST, B.H. (1998). Substrate up-regulation of the human small intestinal peptide transporter, hPepT1. *J. Physiol.,* **507,** 697–706.

WELTMAN, A.C. & ROSE, D.N. (1994). Tuberculosis susceptibility patterns, predictors of multidrug resistance, and implications for initial therapeutic regimens at a New York city hospital. *Arch. Intern. Med.,* **154,** 2161–2167.

WREDEN, C.C., JOHNSON, J., TRAN, C., SEAL, R.P., COPENHAGEN, D.R., REIMER, R.J. & EDWARDS, R.H. (2003). The H^+-coupled electrogenic lysosomal amino acid transporter LYAAT1 localizes to the axon and plasma membrane of hippocampal neurons. *J. Neurosci.,* **23,** 1265–1275.

(Received July 16, 2004
Revised September 10, 2004
Accepted September 20, 2004)